IL NUOVO CIMENTO **44 C** (2021) 108
DOI 10.1393/ncc/i2021-21108-4

COMMUNICATIONS: SIF Congress 2020

Bubble formation in van der Waals crystals: A platform for fundamental studies

E. BLUNDO([1])([*]), C. DI GIORGIO([2]) and G. PETTINARI([3])

([1]) *Physics Department, Sapienza University of Rome - Rome, Italy*
([2]) *Physics Department, University of Salerno - Salerno, Italy*
([3]) *Institute for Photonics and Nanotechnologies, National Research Council - Rome, Italy*

received 15 January 2021

Summary. — van der Waals (vdW) crystals have attracted great interest for the exceptional electronic, optical, chemical, and mechanical properties they reveal in their two-dimensional (2D) form. Furthermore, they are extremely flexible, so that they can be subjected to high strains. Here, we show how micro-scale mechanical deformations in these materials represent an ideal platform to study their fundamental properties. More specifically, we exploit the capability of hydrogen-ion irradiation to induce the formation of 1-layer-thick micro-bubbles, and we also show that their formation can be spatially controlled by litographic approches. These bubbles both modify the opto-electronical properties of the crystal and represent a unique system to study its mechano-elastic and adhesive properties.

1. – Introduction

vdW crystals —such as graphene, hexagonal boron nitride (hBN) and transition metal dichalcogenides (TMDs, *e.g.*, WS_2, WSe_2, MoS_2, $MoSe_2$ and $MoTe_2$)— have attracted great interest due to the possibility to isolate single or few layers. In their 2D form, they exhibit unique properties, that typically differ from those of their bulk counterparts, stemming from enhanced quantum effects and a lowered dielectric screening [1].

While these materials exhibit diverse electronic properties (from the metallic graphene, to the semiconducting TMDs, to the insulating hBN), they are all characterised by similar and exceptional mechanical properties and can withstand tensile strains ∼10–20 % [2]. Since strain can strongly modify their electronic properties [3], great attention has been paid to the development of strategies to deform vdW crystals [4]. Here, we focus our discussion on micro/nano deformations with spherical symmetry and filled with pressurised gas, herein referred to as *domes* or *bubbles*. Such structures host elevated strains (as demonstrated by photoluminescence and Raman studies) [5] and carry relevant information on the mechano-elastic and adhesive properties of the 2D material.

([*]) E-mail: elena.blundo@uniroma1.it

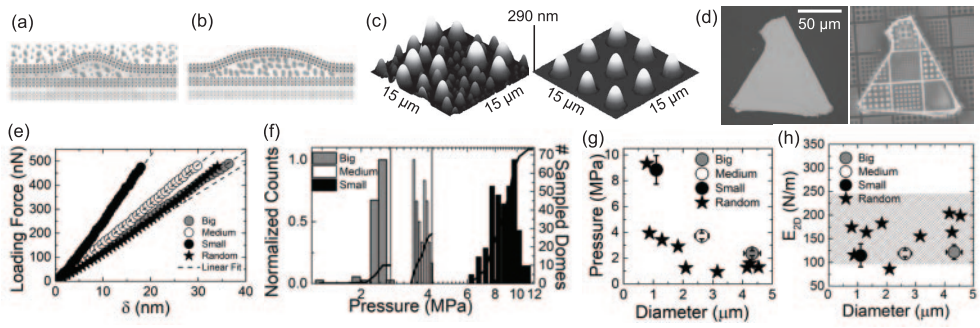

Fig. 1. – (a), (b) Sketch of the H-irradiation process: (a) a bulk flake is irradiated with H ions and the ions penetrate; (b) molecular hydrogen forms in the first interlayer region and coalesces, resulting in the formation of bubbles. Reproduced with permission from TEDESCHI D. *et al.*, *Adv. Mater.* **31** (2019) 1903795. Copyright 2019 WILEY-VCH Verlag GmbH & Co. KGaA, Weinheim. (c) AFM images of randomly formed bubbles and of bubbles created by engineering the formation process. (d) Optical image of a flake before (left) and after (right) the realisation of a H-opaque mask. (e) Typical loading force curves measured on big, medium, and small engineered domes, and on a randomly formed dome. Black dashed lines are linear fits. (f) Pressure distributions for big, medium, and small engineered domes. Black lines are distribution cumulative functions. (g),(h) H_2 pressure (g) and E_{2D} (h) *vs.* dome's diameter for big, medium, and small engineered domes and random domes. The gray patterned area in panel h highlights the range of E_{2D} values reported in the literature. Panels (e)–(h) adapted with permission from DI GIORGIO C. *et al.*, *Adv. Mater. Interfaces*, **7** (2020) 2001024. Copyright 2020 Wiley-VCH GmbH.

2. – Bubbles in 2D materials: Results and discussion

The high flexibility of 2D materials has triggered the search for controllable methods to induce strains. Among them, Tedeschi *et al.* [6] were able to form bubbles in TMDs: A bulk crystal is irradiated with hydrogen (H) ions (typical doses equal to 10^{16}–10^{17} ions/cm^2), which penetrate for one or few layers (fig. 1(a)); H_2 gas forms and coalesces, and H_2-filled bubbles form (fig. 1(b)) [7]. The irradiation is performed with low-energy H-beams (< 20eV) not to damage the crystal [6,8]; Raman studies and the long durability of the bubbles suggest that no sizeable defects are created [6]. A typical atomic force microscopy (AFM) image of MoS_2 bubbles is shown in fig. 1(c), left.

Such bubbles are characterised by interesting properties, such as the fact that their aspect ratio —*i.e.* the ratio between maximum height h_0 and footprint radius R— for each material is constant independently of the bubble size [6, 9, 10]. Indeed, the equilibrium condition for the system can be described by minimising its total energy $U_{tot} = U_{stretch} + U_{adh} + U_{gas}$, where $U_{stretch}$ is the energy related to the elastic deformation of the membrane, U_{adh} takes into account the fact that the membrane is locally detached from the substrate, and U_{gas} is the internal gas energy. For quasi-spherical bubbles

$$U_{adh} = \gamma \cdot \pi R^2, \quad U_{stretch} = A_\nu E_{2D} \cdot \frac{h_0^2}{R^4}, \quad U_{gas} = -B_\nu \Delta p h_0 R^2, \tag{1}$$

where γ is the adhesion energy, E_{2D} is the 2D stretching modulus of the membrane, Δp is the difference between internal and external pressure of H_2, and A_ν and B_ν are positive constants that depend on the Poisson's ratio of the material ν. Contributions related to the bending stiffness are negligible in micron-sized bubbles. By minimising

the $U_{\rm tot}$ both with respect to h_0 and R —to impose equilibrium— one gets

$$\frac{h_0}{R} = C_\nu \cdot \left(\frac{\gamma}{E_{2D}}\right)^{1/4}, \quad \Delta p = D_\nu \cdot \frac{h_0^3}{R^4}, \tag{2}$$

where C_ν and D_ν are constants depending on ν [11, 12]. This shows how the aspect ratio is related to the elastic and adhesive properties of the material, and is constant independently of R or h_0. Indeed, this limits the maximum strain achievable since $\varepsilon_{\rm max} \propto (h_0/R)^2$. However, the aspect ratio can be increased by introducing external forces. This can be achieved by depositing H-opaque masks over the flakes prior to irradiation, as shown in figs. 1(c),(d). The masks can be realised by spinning a negative-tone electronic resist on the whole sample and by patterning it by means of electron beam lithography, see ref. [10]. This procedure allows us to form bubbles with the desired size and position (see panel (d)). Furthermore, if sufficiently thick, the mask acts as a constraint and the resulting structure is characterised by a much larger aspect ratio [10]. For instance, by realising openings with diameter equal to 5 μm, 3 μm and 1 μm —hereinafter referred to as *big*, *medium* and *small*, respectively— we obtained bubbles with h_0/R equal to 0.201 $\pm$ 0.021, 0.216 $\pm$ 0.021 and 0.289 $\pm$ 0.017, respectively, while in spontaneously-formed domes $h_0/R = 0.168 \pm 0.019$. This increased ratio should correspond to an increased gas pressure. To verify this, we performed AFM nano-indentations on both engineered and randomly formed MoS_2 domes. Besides the pressure, these measurements allow us also to measure the stretching modulus E_{2D}. We positioned the AFM tip on the top-most location of each dome and pushed the membrane down for a distance δ, by applying a force $F(\delta)$. Figure 1(e) shows typical $F(\delta)$ curves as acquired on big, medium, and small domes, and on a random one, having a footprint radius similar to the medium dome, but smaller height, for comparison. By employing the same loading force setpoint ($F^{\rm max} \sim 500$ nN), we find a different response depending on both the size and production procedure. For instance, the slope decreases when increasing the radius, thus indicating a size-driven softening, with bigger domes hosting lower inner pressure. On the other hand, the curve acquired on the random bubble discloses two remarkable characteristics: 1) for $\delta \lesssim 20$ nm, a linear behaviour is found, with even smaller slope than the big engineered dome, suggesting a lower pressurisation in the randomly produced bubbles; 2) for $\delta \gtrsim$20 nm the loading force increases more stiffly and the behaviour is no more linear. However, this is not surprising: the dependence of F on δ is indeed expected to undergo a linear to non-linear transition, by increasing the indentation depth δ [13]. Our experiments suggest such a transition being strongly dependent on pressure, thus occurring at lower depths for softer domes. To get out a quantitative estimate of Δp and E_{2D}, we interpreted the results of the indentation experiments by using the solution of the Föppl-von Karman equation for pressurised ultrathin elastic shells clamped to the edge of a circular hole of footprint radius R, in presence of external loading [13]. As detailed in ref. [14], if 1) the pressurisation is sufficiently high [13] and 2) the analysis is limited to a small-indentation range —where the behaviour is linear with slope k— then

$$\Delta p \approx \log(R/R_{tip}) \cdot \frac{h_0 k}{(2\pi A_h A_\tau R^2)}, \qquad E_{2D} \approx \log(R/R_{tip}) \frac{A_h^2 R^2 k}{2\pi A_\tau h_0^2}, \tag{3}$$

where $A_h \approx 0.645$ and $A_\tau \approx 0.438$, for MoS_2 [15], and R_{tip} is the radius of the AFM tip (which can be measured as in ref. [16]). Linear fits of the $F(\delta)$ curves are shown as dashed lines in fig. 1(e) (the fit being limited to $\delta \lesssim$ 20nm for the random domes). We

performed a statistical analysis of loading force curves acquired on 73 small, 27 medium, 10 big domes, plus 9 random domes of varying size. As shown in fig. 1(f),(g), for the engineered domes we find three well separated pressure distributions: The larger pressure found in smaller domes is indeed in agreement with the theoretical predictions (eq. (2)). Furthermore, Δp in the randomly-produced domes is overall lower than the engineered counterparts (see fig. 1(g)), in agreement with the enhanced aspect ratio of the engineered domes. Finally, the E_{2D} measured values overlap (fig. 1(h)) and agree well with the E_{2D} values reported for MoS_2 by other papers [15, 17-19].

In conclusion, we have shown how 2D materials spherically deformed at the micro-scale can represent a unique platform where to investigate intrinsic parameters of the vdW crystals, such as their stretching modulus. Furthermore, using eq. (2) for random domes, we can estimate the adhesion energy ($C_\nu = 2.24$ for MoS_2) [12]: $\gamma \sim$18 meV/Å^2.

* * *

The authors are grateful to A. Polimeni, F. Bobba, T. Yildirim, M. Felici and Y. Lu for their contribution to the results presented in this work.

REFERENCES

[1] Ajayan P., Kim P. and Banerjee K., *Phys. Today*, **69** (2016) 38.
[2] Bertolazzi S., Brivio J. and Kis A., *ACS Nano*, **5** (2011) 9703.
[3] Trainer D. J., Zhang Y., Bobba F., Xi X., Hla S.-W. and Iavarone M., *ACS Nano*, **13** (2019) 8284.
[4] Blundo E., Cappelluti E., Felici M, Pettinari G. and Polimeni A., *Appl. Phys. Rev.*, **8** (2021) 021318.
[5] Blundo E., Felici M., Yildrim T., Pettinari G., Tedeschi D., Miriametro A., Liu B., Ma W., Lu Y. and Polimeni A., *Phys. Rev. Res.*, **31** (2019) 1903795.
[6] Tedeschi D., Blundo E., Felici M., Pettinari G., Liu B., Yildrim T., Petroni E., Zhang C., Zhu Y., Sennato S., Lu Y. and Polimeni A., *Adv. Mater.*, **31** (2019) 1903795.
[7] Blundo E., *Nuovo Cimento C*, **43** (2020) 112.
[8] Abdelnabi M. M. S., Blundo E., Betti M. G., Cavoto G., Placidi E., Polimeni A., Ruocco A., Hu K., Ito Y. and Mariani C., *Nanotechnology*, **32** (2021) 035707.
[9] Khestanova E., Guinea F., Fumagalli L., Geim A. and Grigorieva I., *Nat. Commun.*, **7** (2016) 12587.
[10] Blundo E., Di Giorgio C., Pettinari G., Yildirim T., Felici M., Lu Y., Bobba F. and Polimeni A., *Adv. Mater. Interfaces*, **7** (2020) 200621.
[11] Yue K., Gao W., Huang R. and Liechti K. M., *J. Appl. Phys.*, **112** (2012) 083512.
[12] Blundo E., Yildirim T., Pettinari G. and Polimeni A., *Phys. Rev. Lett.*, **127** (2021) 046101.
[13] Vella D. and Davidovitch B., *Soft Matter* , **13** (2017) 2264.
[14] Di Giorgio C., Blundo E., Pettinari G., Felici M., Lu Y., Cucolo A. M., Polimeni A. and Bobba F., *Adv. Mater. Interfaces*, **7** (2020) 2001024.
[15] Akinwande D., Brennan C. J., Bunch J. S., Egberts P., Felts J. R., Gao H., Huang R., Kim J.-S., Li T., Li Y., Liechti K. M., Lu N., Park H. S., Reed E. J., Wang P., Yakobson B. I., Zhang T., Zhang Y.-W., Zhou Y. and Zhu Y., *Extreme Mech. Lett.*, **13** (2017) 42.
[16] Sader J. E., *Rev. Sci. Instrum.*, **70** (1999) 3967.
[17] Cooper R. C., Lee C., Marianetti C. A., Wei X., Hone J. and Kysa J. W., *Phys Rev. B*, **87** (2013) 035423.
[18] Castellanos-Gomez A., Poot M., Steele G. A., van der Zant H., Agrait N. and Rubio-Bollinger G., *Adv. Mater.*, **24** (2012) 772.
[19] Liu K., Yan Q., Chen M., Fan W., Sun Y., Suh J., Fu D., Lee S., Zhou J., Tongay S., Ji J., Neaton J. B. and Wu J., *Nano Lett.*, **14** (2014) 5097.